Molecules and Cells

Ataxin-2 Dysregulation Triggers a Compensatory Fragile X Mental Retardation Protein Decrease in *Drosophila* C4da Neurons

In Jun Cha[1,2,5], Davin Lee[1,2,5], Sung Soon Park[1,2], Chang Geon Chung[1,2], Seung Yeon Kim[1,2], Min Gu Jo[1,2], Seung Yeol Kim[1,2], Byung-Hoon Lee[2,3], Young-Sam Lee[2,3,4], and Sung Bae Lee[1,2,4,*]

[1]Department of Brain & Cognitive Sciences, Daegu Gyeongbuk Institute of Science & Technology (DGIST), Daegu 42988, Korea, [2]Protein Dynamics-Based Proteotoxicity Control Laboratory, Basic Research Lab, DGIST, Daegu 42988, Korea, [3]Department of New Biology, DGIST, Daegu 42988, Korea, [4]Well Aging Research Center, Division of Biotechnology, DGIST, Daegu 42988, Korea, [5]These authors contributed equally to this work.
*Correspondence: sblee@dgist.ac.kr
https://doi.org/10.14348/molcells.2020.0158
www.molcells.org

Dendrites require precise and timely delivery of protein substrates to distal areas to ensure the correct morphology and function of neurons. Many of these protein substrates are supplied in the form of ribonucleoprotein (RNP) complex consisting of RNA-binding proteins (RBPs) and mRNAs, which are subsequently translated in distal dendritic areas. It remains elusive, however, whether key RBPs supply mRNA according to local demands individually or in a coordinated manner. In this study, we investigated how *Drosophila* sensory neurons respond to the dysregulation of a disease-associated RBP, Ataxin-2 (ATX2), which leads to dendritic defects. We found that ATX2 plays a crucial role in spacing dendritic branches for the optimal dendritic receptive fields in *Drosophila* class IV dendritic arborization (C4da) neurons, where both expression level and subcellular location of ATX2 contribute significantly to this effect. We showed that translational upregulation through the expression of eukaryotic translation initiation factor 4E (eIF4E) further enhanced the ATX2-induced dendritic phenotypes. Additionally, we found that the expression level of another disease-associated RBP, fragile X mental retardation protein (FMRP), decreased in both cell bodies and dendrites when neurons were faced with aberrant upregulation of ATX2. Finally, we revealed that the PAM2 motif of ATX2, which mediates its interaction with poly(A)-binding protein (PABP), is potentially necessary for the decrease of FMRP in certain neuronal stress conditions. Collectively, our data suggest that dysregulation of RBPs triggers a compensatory regulation of other functionally-overlapping RBPs to minimize RBP dysregulation-associated aberrations that hinder neuronal homeostasis in dendrites.

Keywords: Ataxin-2, dendrite, fragile X mental retardation protein, mRNA supply, RNA-binding protein

INTRODUCTION

Due to their complex polarized structure and constant fluctuation of electrophysiological properties, neurons require precise and timely regulation of protein expression in both proximal somatic areas and distal areas. To meet distal demands, neurons employ local translation processes that involve local translation machineries and local supply of mRNAs as a form of ribonucleoprotein (RNP) complex consisting of mRNAs and RNA-binding proteins (RBPs) (Ravanidis et al., 2018). The regulation of mRNA is particularly important for meeting the

Received 24 July, 2020; revised 24 September, 2020; accepted 24 September, 2020; published online 26 October, 2020

eISSN: 0219-1032

proteome demands of dendritic areas as the delivery and processing of local mRNA provides the primary supply of protein substrates in areas where they are most needed. The regulation of mRNA is tightly controlled by RBPs, which mediate mRNA processing, splicing, transportation, translation, and turn-over (Hentze et al., 2018; Kishore et al., 2010). Given the crucial roles of RBPs in meeting local neuronal demands, it is not surprising that their dysregulation results in imbalanced neuron homeostasis, which in turn causes morphological and/or functional neuronal abnormalities, many of which are often associated with various neurological disorders such as neurodegenerative diseases (Conlon and Manley, 2017; Hanson et al., 2012; Romano and Buratti, 2013). Accordingly, extensive studies have revealed imperative roles and regulatory mechanisms associated with RBPs in neurons. For example, the RBP FMRP (encoded by the *FMR1* gene) was found to be critically involved in sensory neuron dendritic branching (Lee et al., 2003). Additionally, under certain conditions of cellular stress, RBPs (including G3BP, eIF3 complex, and poly(A)-binding protein [PABP]) mediate assembly of reversible membrane-less stress granules to arrest local translation in order to conserve energy and minimize stress-related damage (for example, that which may occur as a result of the accumulation of misfolded proteins) (Protter and Parker, 2016). However, it remains elusive whether local protein demands are fulfilled by (1) distinct RBPs acting individually or (2) a coordinated group of RBPs acting in an orchestrated manner.

In this study, we use *Drosophila* larval dendritic arborization (da) neurons to investigate how RBPs respond to the dysregulation of a disease-associated RBP, ATX2. Until recently, ATX2 received great attention as the disease-responsible gene for polyglutamine spinocerebellar ataxia 2 (SCA2) (Lee et al., 2020). However, the mutation of RBP ATX2 has also been implicated in other major neurodegenerative diseases, including Huntington's disease (Xu et al., 2019), amyotrophic lateral sclerosis (Bakthavachalu et al., 2018; Elden et al., 2010; Van Damme et al., 2011), Parkinson's disease (Nkiliza et al., 2016), and Machado-Joseph disease (Ding et al., 2016). Additionally, previous reports indicate that the dysregulation of ATX2 disrupts the interaction of ATX2 with PABP, thereby disturbing cellular processes such as those associated with the circadian rhythm (Lim and Allada, 2013; Zhang et al., 2013). Furthermore, ATX2 is reported to not only stabilize target mRNAs and increase the abundance of their corresponding proteins (Yokoshi et al., 2014), but also to regulate mRNA/protein supply to distal areas by performing its RBP roles (Sudhakaran et al., 2014). Here, we induced dysregulation of ATX2 in larval class IV dendritic arborization (C4da) neurons by overexpressing ATX2 and characterized the neuronal response. We provide evidence that the readjustment of FMRP (another RBP) in both the soma and dendritic areas, may act as a cellular mechanism to rebalance the dysregulated ATX2. Our data suggest that neurons may attempt to achieve local mRNA/proteome homeostasis by stabilizing mRNA regulations through coordinated regulation of RBPs.

MATERIALS AND METHODS

Drosophila stocks

All flies were maintained at 25°C and 60% humidity. The following lines were obtained from Bloomington *Drosophila* Stock Center (USA): w^{1118} (3605), *UAS-luciferase* (35788), *UAS-FMRP RNAi* (34944), *UAS-FMR1* (6931), *UAS-eIF4e1* (8650). *UAS-PABP 3xHA* (F000753) was obtained from FlyORF. *UAS-ATX2* (II), *UAS-flag-dATX2-NLS/UAS-ATX2-NLS* (III), *UAS-flag-dATX2-NES/UAS-ATX2-NES* (II), *UAS-atx2 △ClA3/UAS-ATX2-△PAM2* (III), *FRT82B* $atx2^{X1}$ (III) was provided by Leo. J. Pallanck (University of Washington, USA). The *UAS-FMR1-GFP* (III) line was obtained from F. B. Gao (University of Massachusetts, USA). ppk^{1a}*-Gal4* (III), *UAS-CD4-tdTomato* (III), *UAS-CD4-tdGFP* (III), *Elav-GS-Gal4* (III), *109-Gal4>SOP-FLP, UAS-mCD8GFP* (II), *FRT82B-tub-Gal80* (III), *109-Gal4>UAS-mCD2-RFP* (II), and *Elav-Gal4* (III) was provided by Yuh Nung Jan (University of California–San Francisco, USA).

Generation of Mosaic analysis with a repressible cell marker method (MARCM) and flp-out clones

MARCM analysis of ATX2 mutations was performed by crossing 109-Gal4>SOP-FLP,UAS-mCD8GFP; FRT82B,tub-Gal80 flies (a gift from Yuh Nung Jan) with FRT82B, $atx2^{X1}$ flies to generate marked neurons mutant for ATX2. Wild-type MARCM clones in da neurons were generated using wild-type FRT chromosomes.

Immunohistochemistry (IHC)

As previously described by Park et al. (2020), third instar larvae were dissected and fixed with 3.7% formaldehyde for 20 min at room temperature. After washing with PBST (0.3% Triton-X100 in phosphate-buffered saline), the larval fillets were incubated in a blocking buffer for 1 h at room temperature (RT). Next, the fillets were incubated in the primary antibody overnight at 4°C. α-Datx2 antibody from Leo. J. Pallanck (1:2,000) was used to detect ataxin-2. Fillets were then washed with washing buffer three times for 5 min each. Then, they were further incubated in the secondary antibody for 3 h at room temperature. The following secondary antibodies were used: goat α-rabbit Alexa 647 (A21244, 1:200; Invitrogen, USA) and goat α-Horseradish Peroxidase (123-545-021, 1:200; Jackson ImmunoResearch, USA). Fillets were washed five times with washing buffer prior to mounting on a slide glass for imaging. 70% PBG (70% Glycerol in PBS) was used as a mounting solution.

Confocal microscopy

Images of larvae fillet after IHC and live third instar larvae were obtained using Zeiss LSM700, LSM780 and LSM800 confocal microscopy (Zeiss, Germany). All images of the C4da neurons were acquired from abdominal A2-A6 segments.

Image processing

Images obtained from confocal microscopy were processed using Zen black program, Adobe Photoshop CC and ImageJ. All images presented in the same panel were processed in the same manner.

Reverse transcription polymerase chain reaction (RT-PCR)

Total RNA was extracted from the heads of *Drosophila* with the following genotypes: w^{1118}/*Elav-GS-gal4* and *UAS-ATX2*/*Elav-GS-gal4*. Concentration of total RNA of each sample was measured by NanoDrop 2000 spectrophotometer (Thermo Fisher Scientific, USA). Rp49 RNA was used as a reference for normalizing *FMR1* mRNA level.

Primer sequences for *dFMR1*:

5'– CACTCACCCGCATACACGAATA
3'– TTGTGTTCAATGCTCCTCTCCC

Primer sequences for *ATX2*:

5'– GCACATTCTCGGGCAACTTT
3'– CGTTGGCGGCACTATCCAAT

Dendrite analysis

All images of dendrites were first preprocessed to remove noise using ImageJ. Then, those images were used to analyze dendritic branch orders using the dendritic shaft order method (Neurolucida; MBF Bioscience, USA). Dendrites were also categorized into 4 different groups based on the relative

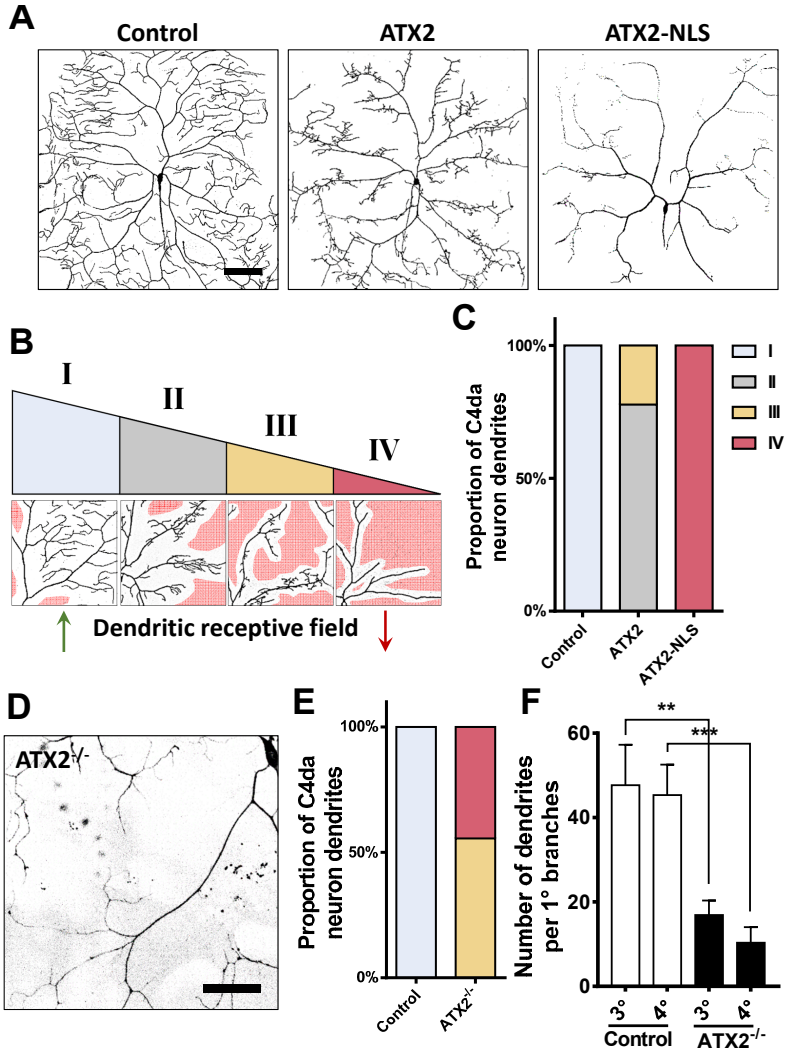

Fig. 1. ATX2 is associated with the regulation of both dendritic terminals and receptive field coverage in *Drosophila* C4da neurons. (A) Representative images of dendrites of C4da neurons of Control or expressing denoted ATX2 transgenes (Genotype: Control, *+/+; ppk^{1a}>UAS-CD4-tdTom/UAS-luciferase;* ATX2, *UAS-ATX2/+; ppk^{1a}>UAS-CD4-tdTom/+;* ATX2-NLS, *UAS-flag-ATX2 NLS/+; ppk^{1a}>UAS-CD4-tdTom/+*). Scale bar = 100 μm. (B) A schematic image illustrating how dendrites are grouped into similar level of dendritic receptive fields. Below are representative images of ATX2-induced dendritic phenotypes and their corresponding groups. (C) Quantification of dendritic receptive fields of neurons expressing denoted ATX2 transgenes described in Fig. 1A. (D) Representative image of dendrites of C4da neurons with ATX2 knockout genes (Genotype: ATX2$^{-/-}$, *109-Gal4>SOP-FLP, UAS-mCD8GFP/+; FRT82B, atx2X1/FRT82B, tub-Gal80*). Scale bar = 20 μm. (E) Quantification of dendritic receptive fields of neurons expressing denoted ATX2 transgenes described in Fig. 1D and (Genotype: Control, *+/+; ppk^{1a}>UAS-CD4-tdTom/UAS-luciferase*). (F) Quantification of the dendritic branches of neurons expressing denoted ATX2 transgenes described in Figs. 1D and 1E. $^{**}P < 0.01$, $^{***}P < 0.01$ by two-tailed *t*-test; error bar ± SEM; n ≥ 3 neurons.

severity of loss of dendritic receptive field.

Sholl analysis of dendritic arbors of C4da neurons

Concentric circles with 10-μm increments were drawn around the soma, and the number of dendritic branches that intersected each circle was counted. Dendrites of C4da neurons were analyzed with ImageJ.

Statistical analysis

Statistical analysis was done using GraphPad Prism 7 (GraphPad Software, USA). Depending on the data, we applied either Student's *t*-test or one-way ANOVA followed by Tukey's post-hoc analysis. In all figures, n.s., *, **, ***, and **** represent $P > 0.05$, $P < 0.05$, $P < 0.01$, $P < 0.001$, and $P < 0.0001$, respectively. Error bars are SEM.

RESULTS

ATX2 is associated with the regulation of both dendritic terminals and receptive field coverage in *Drosophila* C4da neurons

To investigate how RBPs respond to dysregulated ATX2, we first examined the functional role of ATX2 in the regulation of dendritic structures. To this end, we expressed three different transgenes of ATX2 (ATX2, ATX2-NES, ATX2-NLS) in in *Drosophila* C4da neurons and observed the consequent dendritic phenotypes. A membrane marker (CD4-tdTomato) was used to visualize dendritic morphology. By immunostaining overexpressed ATX2 with an anti-ATX2 antibody, we confirmed that full length ATX2 and ATX2 with exogenous nuclear exit signal (ATX2-NES) predominantly localize in the cytoplasm, while ATX2 with an exogenous nuclear localizing signal (ATX2-NLS) predominantly localizes in the nucleus of C4da neurons (Supplementary Fig. S1A), as previously shown in dorsal neurons (Zhang et al., 2013). In addition to sharing similar localization patterns, ATX2 and ATX2-NES showed comparable dendritic phenotypes (Supplementary Fig. S1B). Thus, we decided to further characterize dendritic phenotypes induced by ATX2 and ATX2-NLS only. We noticed that ATX2 and ATX2-NLS exhibit obvious reduction in dendritic receptive field (Fig. 1A). To quantitatively assess the level of reduction in dendritic receptive field, we categorized dendritic phenotypes into 4 different groups (as specified in Fig. 1B) based on relative severity. Compared to control C4da neurons, ATX2- and ATX2-NLS-expressing neurons exhibited higher proportions in groups II, III, and IV (Fig. 1C). As shown in Fig. 1C, a higher proportion of ATX2-NLS-expressing neurons were assigned to group IV compared to ATX2-expressing neurons, indicating that ATX2-NLS displays a more severe reduction in dendritic receptive field. We next questioned whether the lack of ATX2 could also bring about changes in the pattern of dendritic terminals. Considering the second instar larval lethality associated with a homozygous knockout of ATX2 (Satterfield et al., 2002), we utilized the MARCM to specifically knockout ATX2 in *Drosophila* C4da neurons. $ATX2^{-/-}$ C4da neurons displayed higher proportions of group III and IV dendrites accompanied by significantly reduced number of higher order dendritic branches (Figs. 1D-1F). Collectively, our data indicate that C4da neurons maintain stereotypical morphology that ensures optimized coverage of dendritic receptive field when provided with a properly regulated amount of ATX2 protein.

ATX2 and translational regulator eukaryotic translation initiation factor 4E (eIF4E) cooperate to alter dendritic terminals

Next, we questioned how ATX2 is associated with the regulation of terminal dendrites. Given the fact that ATX2 binds to and/or regulates the stability and translation of more than 4,000 RNA molecules (Yokoshi et al., 2014), we hypothesized that the role of ATX2 in modifying dendritic morphology may be associated with its regulatory role in local mRNA supply.

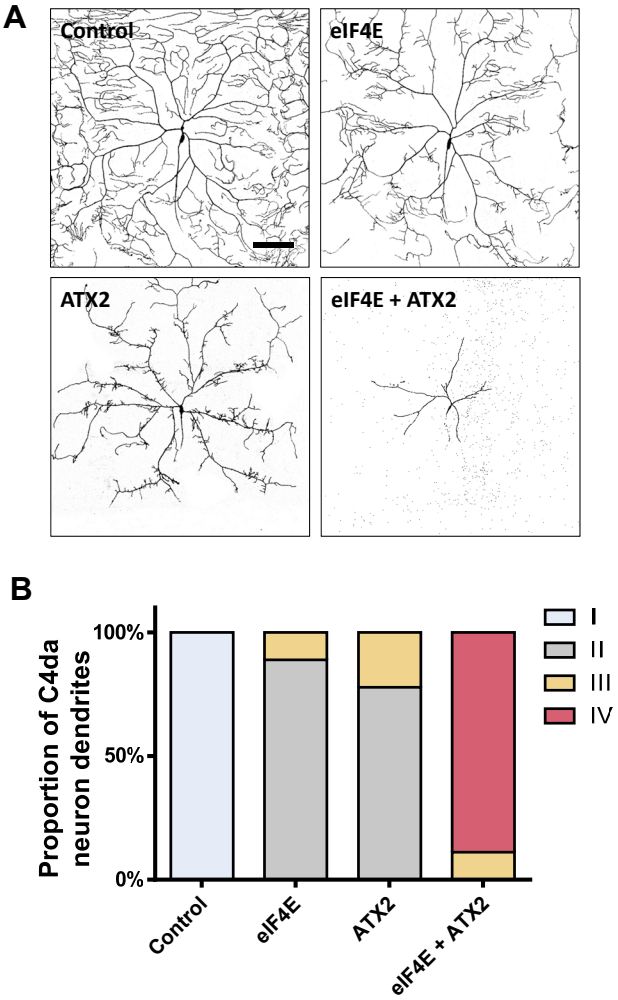

Fig. 2. ATX2 and translational regulator eIF4E cooperate to alter dendritic terminals. (A) Representative images of dendrites of C4da neurons of Control or expressing denoted transgenes (Genotype: Control, *+/+; ppk^{1a}>UAS-CD4-tdTom/UAS-luciferase*; eIF4E, *UAS-eIF4e1/+; ppk^{1a}>UAS-CD4-tdTom/+*; ATX2, *UAS-ATX2/+; ppk^{1a}>UAS-CD4-tdTom/+*; eIF4E + ATX2, *UAS-eIF4e1/UAS-ATX2; ppk^{1a}>UAS-CD4-tdTom/+*). Scale bar = 100 μm. (B) Quantification of dendritic receptive fields of neurons expressing denoted ATX2 transgenes described in Fig. 2A.

To experimentally validate this hypothesis, we promoted translational efficiency in C4da neurons by overexpressing eIF4E, a eukaryotic translation initiation factor involved in directing ribosomes to the cap structure of mRNAs (Gingras et al., 1999), and observed the effect on dendritic morphology. While the overexpression of eIF4E induced marginal changes in dendritic morphology, the co-overexpression of ATX2 and eIF4E further enhanced the ATX2-induced dendritic phenotypes (Fig. 2). Notably, a previous study showed that ATX2 forms a complex with eIF4E together with PABP and eIF4G to function cooperatively (Lastres-Becker et al., 2016; Nonhoff et al., 2007), which appears to be consistent with our result showing their cooperation in the regulation of dendrite morphology. These data demonstrate that the cooperation between RBPs ATX2 and translational regulator eIF4E acts to alter the dendritic terminals.

Decrease in FMRP level is a neuronal compensatory response to the aberrant upregulation of ATX2

Next, we questioned how neurons accommodate for the change in RNA pool upon upregulating ATX2. We hypothesized that neurons might readjust expression levels of other RBPs as a compensatory response to the potential dysregulation of mRNAs induced by ATX2. To test this hypothesis, we first looked for potential RBP binding partners of ATX2 by searching through previous literature and available databases; we identified FMRP as a likely candidate due to its functional overlap with ATX2 (Sudhakaran et al., 2014). Previous reports indicate that the RBP FMRP, which plays a key role in protein regulation, translation, and RNP assembly (Eberhart et al., 1996), physically binds to and functions with ATX2 to form complexes that organize neuronal translational control (Sudhakaran et al., 2014). Therefore, we tested whether the dysregulation of ATX2 can affect FMRP distribution and/or

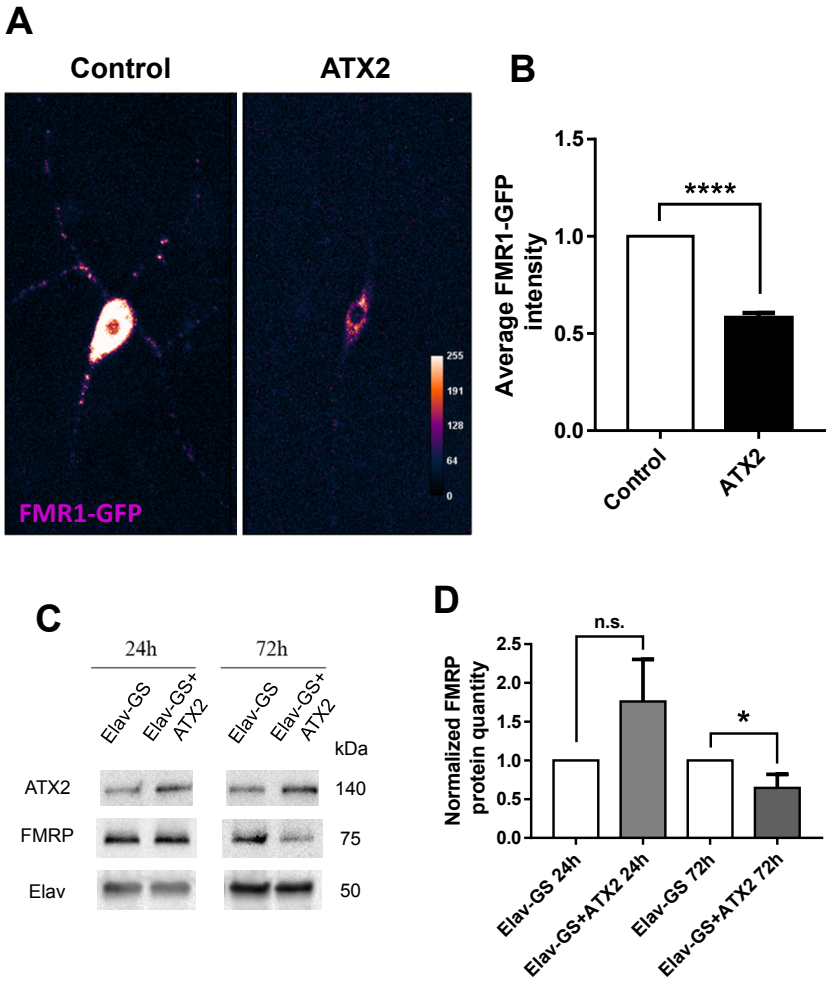

Fig. 3. Aberrant upregulation of ATX2 decreases neuronal FMRP protein levels. (A) Representative images of FMR1-GFP in C4da neurons of Control or ATX2 expressing neurons (Genotype: Control, *+/+; ppk^{1a}-Gal4/UAS-FMR1-GFP*; ATX2, *UAS-ATX2/+; ppk^{1a}-Gal4/UAS-FMR1-GFP*). (B) Quantification of the average FMR1-GFP intensity in C4da neurons expressing denoted transgenes described in Fig. 3A. ****$P < 0.0001$ by two-tailed *t*-test; error bars ± SEM; n ≥ 9 neurons. (C) The amount of protein level of ATX2 and FMRP after 24 h or 72 h of RU486 treatment in the brain of Control or expressing ATX2 (Genotype: Elav-GS, +/+; *elav-GS-Gal4*/+; Elav-GS + ATX2, *UAS-ATX2*/+; *elav-GS-Gal4*/+). (D) Quantification of the protein level of FMRP. The values were normalized by those of Elav protein expression. n.s., not significant; *$P = 0.0249$ by two-tailed *t*-test; error bars ± SEM; n = 3 replicates.

abundance in C4da neurons. To address this issue, we utilized a GFP-tagged FMRP (FMR1-GFP) to observe the consequent changes in distribution pattern and amount of FMRP. Surprisingly, ATX2 expression resulted in a marked reduction in the overall intensity of FMR1-GFP in the soma and an almost complete ablation of dendritic FMRP puncta (Figs. 3A and 3B). To comprehensively characterize the ATX2-associated decrease of FMRP, we measured the mRNA and protein level of endogenous *FMR1* and FMRP, respectively, at two different time points (24 h and 72 h) following induction of pan-neuronal ATX2 overexpression using the inducible GeneSwitch method in *Drosophila* brains. While ATX2 overexpression did not alter the mRNA level of *FMR1* in neurons at either time point (Supplementary Fig. S2), the protein level of FMRP decreased significantly only after 72 h of RU486 treatment inducing ATX2 overexpression (Figs. 3C and 3D), suggesting that the ATX2-induced reduction of FMRP may not be a temporally acute cellular event. These data show that ATX2 dysregulation can affect the amount and likely the distribution of another RBP, FMRP, as a potential mode of interplay between the two RBPs.

Next, we questioned how the reduction in FMRP level contributes to the ATX2-induced dendritic phenotypes. Decreased FMRP level might be a pathogenic feature of or a compensatory response to the ATX2 dysregulation. To distinguish between these possibilities, we first overexpressed

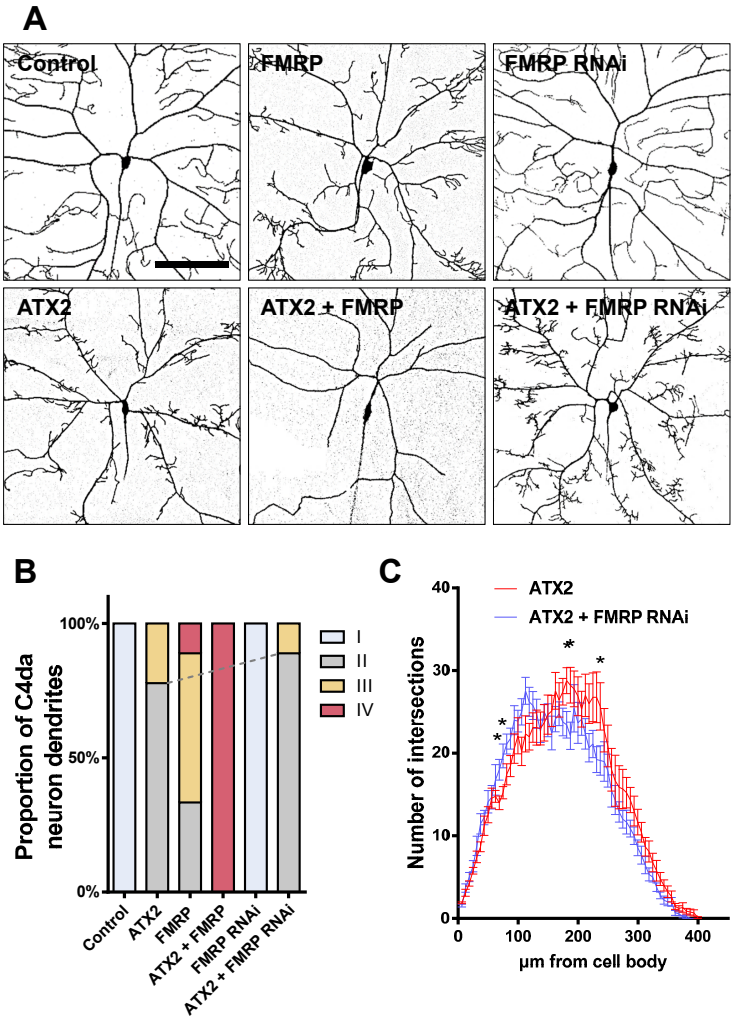

Fig. 4. Decrease in FMRP level is a neuronal compensatory response to the aberrant upregulation of ATX2. (A) Representative images of dendrites of C4da neurons of Control or expressing denoted transgenes (Genotype: Control, *+/+; ppk^{1a}>UAS-CD4-tdTom/UAS-luciferase*; FMRP, *+/+; ppk^{1a}>UAS-CD4-tdTom/UAS-FMR1*; FMRP RNAi, *+/+; ppk^{1a}>UAS-CD4-tdTom/UAS-FMRP RNAi*, ATX2, *UAS-ATX2/+; ppk^{1a}>UAS-CD4-tdTom/UAS-luciferase*; ATX2 + FMRP, *UAS-ATX2/+; ppk^{1a}>UAS-CD4-tdTom/UAS-FMR1*; ATX2 + FMRP RNAi, *UAS-ATX2/+; ppk^{1a}>UAS-CD4-tdTom/UAS-FMRP RNAi*). Scale bar = 100 μm. (B) Quantification of dendritic receptive fields of neurons expressing denoted transgenes described in Fig. 4A. Gray-dotted line indicates the differences in group II and III catagorized dendrite proportions of ATX2 and ATX2 + FMRP RNAi expressing C4da neurons. (C) A sholl analysis of C4da neuron dendrites in 3rd instar larvae expressing the denoted transgenes (Genotype: ATX2, *UAS-ATX2/+; ppk^{1a}>UAS-CD4-tdTom/UAS-luciferase*; ATX2 + FMRP RNAi, *UAS-ATX2/+; ppk^{1a}>UAS-CD4-tdTom/UAS-FMRP RNAi*). $*P < 0.05$ by two-tailed *t*-test; error bars ± SEM; n = 9 replicates.

FMRP with or without ATX2 overexpression in C4da neurons, and examined the consequent dendritic phenotypes. We found that the dendritic phenotypes induced by overexpression of FMRP were comparable to those induced by overexpression of ATX2 (Figs. 4A and 4B). The co-overexpression of FMRP and ATX2 resulted in the enhanced reduction of dendritic receptive field, suggesting that the two RBPS interact to regulate dendritic morphology. Next, we tested whether further decrease in FMRP level could suppress ATX2-induced dendritic phenotypes. The expression of FMRP RNAi did not alter the morphology of dendrites in C4da neurons (Figs. 4A and 4B). However, FMRP RNAi resulted in the reduced proportion of group III accompanied by increased proportion of group II in C4da neurons overexpressing ATX2, indicative of the partial suppression of ATX2-induced dendritic phenotypes (Fig. 4B, gray-dotted line). We next analyzed the dendritic arbors of C4da neurons either expressing ATX2 alone or co-expressing ATX2 and FMRP RNAi. Upon examining den-

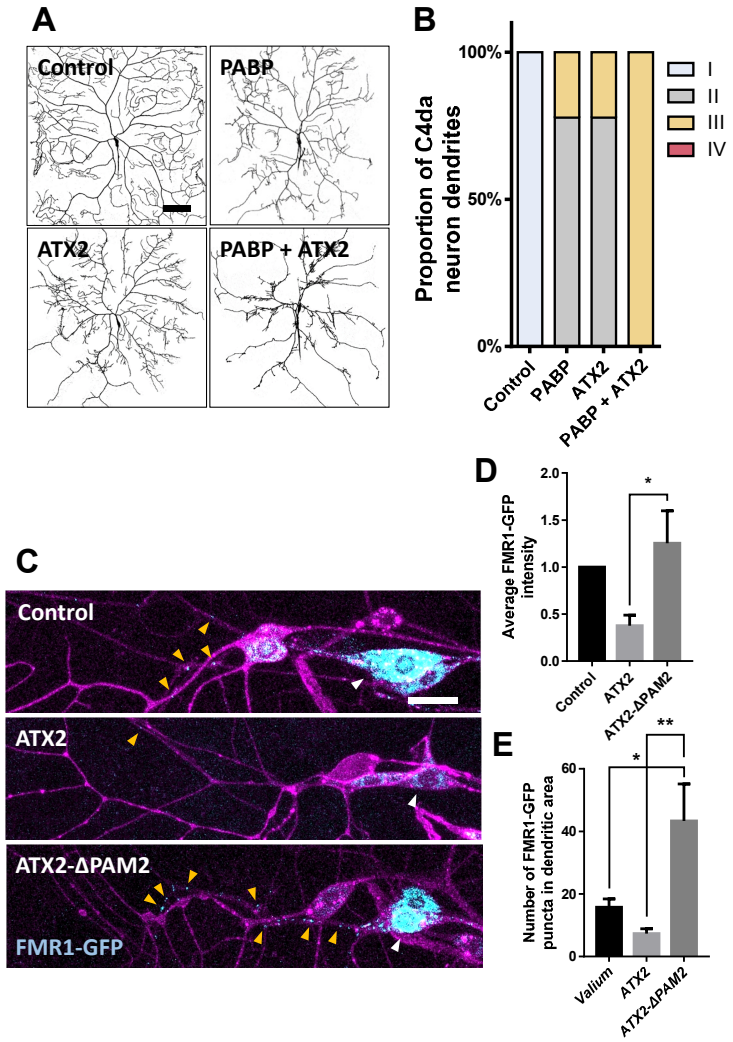

Fig. 5. Dendritic ATX2 toxicity requires its interactions with co-factors through the PAM2 motif. (A) Representative images of dendrites of C4da neurons of Control or expressing denoted transgenes (Genotype: Control, *+/+; ppk^{1a}>UAS-CD4-tdTom/UAS-luciferase*; PABP, *+/+; ppk^{1a}>UAS-CD4-tdTom/UAS-PABP 3xHA*; ATX2, *UAS-ATX2/+; ppk^{1a}>UAS-CD4-tdTom/UAS-luciferase*; PABP + ATX2, *UAS-ATX2; ppk^{1a}>UAS-CD4-tdTom/UAS-PABP 3xHA*). Scale bar = 100 μm. (B) Quantification of dendritic receptive fields of neurons expressing denoted transgenes described in Fig. 5A. (C) Representative images of FMR1-GFP (cyan) in da neuron clusters (magenta) expressing denoted transgene (Genotype: Control, *109(2)80-Gal4>UAS-mCD2-RFP/+; UAS-FMR1-GFP/UAS-luciferase*; ATX2, *109(2)80-Gal4>UAS-mCD2-RFP/UAS-ATX2; UAS-FMR1-GFP/+*; ATX2-ΔPAM2, *109(2)80-Gal4>UAS-mCD2-RFP/+; UAS-FMR1-GFP/UAS-atx2 △CIA3*). Scale bar = 20 μm. White arrowheads refer to FMR1-GFP in somatic areas while yellow arrowheads refer to dendritic FMR1-GFP punctae. (D) Quantification of the average FMR1-GFP intensity in somatic C4da neurons expressing denoted transgenes described in Fig. 5C. $*P < 0.05$ by one-way ANOVA with Tukey's post-hoc correction. n ≥ 9 neurons. (E) Quantification of the number of FMR1-GFP puncta in dendritic areas in C4da neurons expressing denoted transgenes described in Fig. 5C. $*P < 0.05$, $**P < 0.01$ by one-way ANOVA with Tukey's post-hoc correction. n ≥ 9 neurons.

dritic arbors using sholl analysis, interestingly, we found that a significant shift in dendritic branching close to the somatic areas occurred (Fig. 4C), indicating that FMRP RNAi may ameliorate dendritic branching abnormalities caused by aberrant upregulation of ATX2 particularly in regions proximal to somatic areas. The relatively weak effect of FMRP RNAi on ATX2-induced dendritic abnormalities may be due to the compensatory reduction of FMRP in response to aberrant upregulation of ATX2, which reduced the effectiveness of the FMRP RNAi on the expression level of *FMR1*. Together, these data suggest that FMRP level is reduced in C4da neurons to potentially compensate for the upregulation of ATX2 that induces aberrant reduction of dendritic receptive field.

PABP and the PAM2 motif of ATX2 are involved in the compensatory neuronal response to the aberrant upregulation of ATX2

Next, we sought to further characterize molecular mechanism of the compensatory neuronal response to the aberrant upregulation of ATX2. Notably, a previous study on ATX2 toxicity using the *Drosophila* eye system highlighted the importance of the PABP-interacting motif (PAM2) in mediating ATX2 toxicity (Lessing and Bonini, 2008). In addition, previous studies showed that ATX2 forms a complex with PABP, through the PAM2 motif, together with eIF4G that constitutes the translational initiator complex with eIF4E as a core component to modulate neuronal translation (Gruner et al., 2016). Thus, we examined whether the upregulation of PABP with ATX2 could further exacerbate the ATX2-induced dendritic alterations. We found similar dendritic phenotypes between C4da neurons overexpressing PABP and those overexpressing ATX2 (Figs. 5A and 5B). However, co-overexpression of ATX2 with PABP intensified ATX2-induced dendritic phenotypes; more neurons were categorized into group III (Fig. 5B), indicating an exacerbation of ATX2-induced dendritic alterations. Next, we decided to examine whether the PAM2 motif of ATX2 was associated with the compensatory decrease of FMRP. To this end, we overexpressed ATX2 or ATX2-ΔPAM2 together with FMR1-GFP in dorsal clusters of da neurons and observed the expression pattern and amount of FMR1-GFP. Interestingly, while the overexpression of ATX2 greatly reduced the FMR1-GFP levels in dorsal clusters of da neurons, the overexpression of ATX2-ΔPAM2 did not significantly alter the expression level of FMR1-GFP (Figs. 5C-5E). Consistently, the number of dendritic FMR1-GFP puncta was greatly reduced in ATX2-expressing neurons, but not in ATX2-ΔPAM2-expressing neurons, compared to the control (Fig. 5E). The obvious difference between ATX2 and ATX2-ΔPAM2-expressing neurons in the distribution of FMR1-GFP suggests that the PAM2 motif is involved in the compensatory neuronal response to conditions of high neuronal stress, such as that represented by the aberrant upregulation of multiple local RBPs.

DISCUSSION

In this study, we provide experimental evidences that support the potential presence of the interplay between ATX2 and FMRP for the regulation of dendritic morphology (Supplementary Fig. S3). Although we found that the dysregulation of ATX2 led to dendritic abnormalities, how ATX2 dysregulation leads to dendritic alterations, how ATX2 induction leads to decrease in neuronal FMRP, or how the readjustment of FMRP contributes to ATX2-induced dendritic phenotype is yet to be fully understood.

Although we presented dendritic phenotypes associated with deletion of ATX2, most of this study examined the effects of overexpressed ATX2 only. Interestingly, intermediate polyQ repeats in ATX2 increases the risk for ALS (Elden et al., 2010). In that seminal paper, the authors showed that intermediate polyQ repeats in ATX2 increased its stability and/or limited its degradation, thereby increasing the effective concentration of ATX2, ultimately promoting TDP-43 pathology. Thus, the dendritic phenotypes we characterized in this paper may be pertinent to disease-associated pathology, as both ATX2 with intermediate repeats and overexpressed ATX2 increase its effective concentration.

How might ATX2 dysregulation lead to dendritic alterations? A previous study indicates that ATX2 binds to and/or regulates the stability and translation of more than 4,000 RNA molecules (Yokoshi et al., 2014), suggesting that aberrant upregulation of ATX2 can induce dysregulation of mRNA homeostasis in neurons. Additionally, ATX2 was previously reported to be involved in local translation of mRNAs (Sudhakaran et al., 2014) and is known to form a complex with eIF4E in neurons (Lastres-Becker et al., 2016). This raises the possibility that the ATX2-induced dendritic phenotypes observed in our study may be associated with changes in local translation of mRNAs. Consistent with this possibility, we found that the co-overexpression of ATX2 with eIF4E further enhanced the reduction of dendritic receptive fields. Given the huge number of ATX2 mRNA targets that cover a broad range of functions (Yokoshi et al., 2014), multiple targets are likely to be involved in altering the dendritic receptive field. Therefore, to understand the mechanistic details of how ATX2 affects dendritic receptive fields, it may be useful to identify downstream mRNAs and/or proteins whose expression levels or activation statuses are changed and so may contribute to ATX2-induced dendritic morphology.

We found that the dysregulation of ATX2 led to the decrease of FMRP in both somatic and distal dendritic area in *Drosophila* C4da neurons. There are two pathways associated with protein homeostasis that may explain the observed decrease in FMRP with no change in the FMR1 mRNA level: downregulated translation or upregulated degradation of FMRP. As ATX2 is able to either activate or inactivate neuronal mRNA translation depending on the neuronal context (McCann et al., 2011; Sudhakaran et al., 2014), the dysregulation of ATX2 can induce downregulated translation of FMRP in our neuronal system. However, we have not noticed any decrease in the level of Elav protein in western blot nor the intensity of CD4-tdTomato on C4da neuronal membranes upon ATX2 overexpression. These data suggest that global translational inhibition by ATX2 did not occur in our system. On the other hand, it is also possible that ATX2 dysregulation induces upregulated degradation of FMRP. A previous study showed that dephosphorylated FMRP is prone to be degraded through the ubiquitin proteasome system (UPS),

with particular rapidity in neuronal dendrites (Nalavadi et al., 2012). Thus, it may be interesting to test whether ATX2 dysregulation induces either downregulated translation of FMRP or upregulated degradation of FMRP through changes in the phosphorylation status of FMRP.

Furthermore, we speculate that the compensatory adjustment of the amount of FMRP may be affected by the condition of the neuronal context. We showed that the ATX2-induced decrease of overexpressed FMR1-GFP was associated with the PAM2 motif of ATX2 (Figs. 5C-5E). However, considering the difference in the expression levels of ATX2 and ATX2-ΔPAM2, the decrease in the amount of endogenous FMRP was not obviously different between fly brains overexpressing ATX2 and those overexpressing ATX2-ΔPAM2 (Supplementary Figs. S4 and S5). These data suggest that the functional role of the PAM2 motif in the compensatory neuronal response may differ depending on the relative strength of neuronal stress caused by the aberrant upregulation of RBPs, as exemplified by the functional role of the PAM2 motif in the highly stressed neuronal context induced by co-overexpression of functionally-overlapping ATX2 and FMR1-GFP (Figs. 5C-5E). Thus, focused studies on the context-dependent shift in the compensatory readjustment of functionally-overlapping RBPs should be done in the future.

As suggested in Figs. 4 and 5, our model proposes that neurons may compensate for the dysregulation of mRNA and RBPs by adjusting various other local RBPs. An important question then is how FMRP downregulation confers compensation to the aberrant upregulation of ATX2. A hint to this question may be obtained from a study that showed large functional overlap between ATX2 and FMRP. Sudhakaran et al. (2014) showed that both disease- and RNA-associated proteins, ATX2 and FMRP, have similar *in vivo* functions such as synaptic plasticity, RNA regulation, and mRNP assembly, potentially because they regulate common mRNAs. Thus, it seems possible that the effect of ATX2 and FMRP on the dendrite morphology may primarily involve their RNA-binding abilities mediated by their unique RNA-binding domains, such as the Like-Sm (Lsm)/Lsm-associated domain (LsmAD) in ATX2 and the RNA-binding domains (one RGG domain and two KH domains) in FMRP (Ashley et al., 1993; Siomi et al., 1993).

Finally, we showed that the ATX2-induced dendritic phenotype was further enhanced when co-expressed with FMRP (Figs. 4A and 4B), suggesting that neuronal pathology can be induced by impaired compensatory readjustment of RBPs that attempt to ameliorate the damage of neuronal homeostasis caused by dysregulation of one RBP. Results from a previous study in which ATX2 was identified as a positive modifier of TDP-43 toxicity (Elden et al., 2010), a hallmark for ALS (Heyburn and Moussa, 2017; Neumann et al., 2006), are consistent with our notion since, like ATX2, TDP-43 is involved in several aspects of RNA metabolism, including transcription, alternative splicing and RNA stability (Paulson et al., 2017). We hope that our hypothesis, once further studied, can not only be extended to be the basis for identifying additional potential compensatory mechanisms involving RBPs and/or protein substrates, but also be the structural framework in which we use to understand what pathological consequences may occur when endogenous compensatory mechanisms break down.

Note: Supplementary information is available on the Molecules and Cells website (www.molcells.org).

ACKNOWLEDGMENTS

This work was funded by Basic Science Research Program through the National Research Foundation of Korea, funded by the Ministry of Science and ICT (2018R1A2B6001607 and 2019R1A4A1024278) (to SBL); the Development of Platform Technology for Innovative Medical Measurements Program from the Korea Research Institute of Standards and Science Grant (KRISS-2019-GP2019-0018) (to SBL); and KBRI basic research program through Korea Brain Research Institute funded by Ministry of Science and ICT (20-BR-04-02) (to SBL). The funders had no role in study design, data collection and analysis, decision to publish, or preparation of the manuscript.

AUTHOR CONTRIBUTIONS

D.L., C.G.C., and S.B.L. wrote the manuscript. I.J.C., D.L., S.S.P., S.Y.K., M.G.J., and S.Y.K. performed experiments. D.L., S.Y.K., and M.G.J. analyzed the data. Y.S.L., B.H.L., and S.B.L. provided expertise and feedback. S.B.L. supervised the research.

CONFLICT OF INTEREST

The authors have no potential conflicts of interest to disclose.

ORCID

In Jun Cha	https://orcid.org/0000-0001-7950-3804
Davin Lee	https://orcid.org/0000-0002-1506-5304
Sung Soon Park	https://orcid.org/0000-0001-6576-0922
Chang Geon Chung	https://orcid.org/0000-0001-8155-4926
Seung Yeon Kim	https://orcid.org/0000-0002-7553-2795
Min Gu Jo	https://orcid.org/0000-0002-5565-5018
Seung Yeol Kim	https://orcid.org/0000-0002-9880-2495
Byung-Hoon Lee	https://orcid.org/0000-0002-7101-0471
Young-Sam Lee	https://orcid.org/0000-0002-4702-0127
Sung Bae Lee	https://orcid.org/0000-0002-8980-6769

REFERENCES

Ashley, C.T., Jr., Wilkinson, K.D., Reines, D., and Warren, S.T. (1993). FMR1 protein: conserved RNP family domains and selective RNA binding. Science *262*, 563-566.

Bakthavachalu, B., Huelsmeier, J., Sudhakaran, I.P., Hillebrand, J., Singh, A., Petrauskas, A., Thiagarajan, D., Sankaranarayanan, M., Mizoue, L., Anderson, E.N., et al. (2018). RNP-granule assembly via Ataxin-2 disordered domains is required for long-term memory and neurodegeneration. Neuron *98*, 754-766.e4.

Conlon, E.G. and Manley, J.L. (2017). RNA-binding proteins in neurodegeneration: mechanisms in aggregate. Genes Dev. *31*, 1509-1528.

Ding, D., Li, K., Wang, C., Chen, Z., Long, Z., Peng, Y., Zhou, X., Peng, H., Qiu, R., Xia, K., et al. (2016). ATXN2 polymorphism modulates age at onset in Machado-Joseph disease. Brain *139*, e59.

Eberhart, D.E., Malter, H.E., Feng, Y., and Warren, S.T. (1996). The fragile X mental retardation protein is a ribonucleoprotein containing both nuclear localization and nuclear export signals. Hum. Mol. Genet. *5*, 1083-1091.

Elden, A.C., Kim, H.J., Hart, M.P., Chen-Plotkin, A.S., Johnson, B.S., Fang, X., Armakola, M., Geser, F., Greene, R., Lu, M.M., et al. (2010). Ataxin-2 intermediate-length polyglutamine expansions are associated with increased risk for ALS. Nature *466*, 1069-1075.

Gingras, A.C., Raught, B., and Sonenberg, N. (1999). eIF4 initiation factors: effectors of mRNA recruitment to ribosomes and regulators of translation. Annu. Rev. Biochem. *68*, 913-963.

Gruner, S., Peter, D., Weber, R., Wohlbold, L., Chung, M.Y., Weichenrieder, O., Valkov, E., Igreja, C., and Izaurralde, E. (2016). The structures of eIF4E-eIF4G complexes reveal an extended interface to regulate translation initiation. Mol. Cell *64*, 467-479.

Hanson, K.A., Kim, S.H., and Tibbetts, R.S. (2012). RNA-binding proteins in neurodegenerative disease: TDP-43 and beyond. Wiley Interdiscip. Rev. RNA *3*, 265-285.

Hentze, M.W., Castello, A., Schwarzl, T., and Preiss, T. (2018). A brave new world of RNA-binding proteins. Nat. Rev. Mol. Cell Biol. *19*, 327-341.

Heyburn, L. and Moussa, C.E. (2017). TDP-43 in the spectrum of MND-FTLD pathologies. Mol. Cell. Neurosci. *83*, 46-54.

Kishore, S., Luber, S., and Zavolan, M. (2010). Deciphering the role of RNA-binding proteins in the post-transcriptional control of gene expression. Brief. Funct. Genomics *9*, 391-404.

Lastres-Becker, I., Nonis, D., Eich, F., Klinkenberg, M., Gorospe, M., Kotter, P., Klein, F.A., Kedersha, N., and Auburger, G. (2016). Mammalian ataxin-2 modulates translation control at the pre-initiation complex via PI3K/mTOR and is induced by starvation. Biochim. Biophys. Acta *1862*, 1558-1569.

Lee, A., Li, W., Xu, K., Bogert, B.A., Su, K., and Gao, F.B. (2003). Control of dendritic development by the Drosophila fragile X-related gene involves the small GTPase Rac1. Development *130*, 5543-5552.

Lee, D., Lee, Y.I., Lee, Y.S., and Lee, S.B. (2020). The mechanisms of nuclear proteotoxicity in polyglutamine spinocerebellar ataxias. Front. Neurosci. *14*, 489.

Lessing, D. and Bonini, N.M. (2008). Polyglutamine genes interact to modulate the severity and progression of neurodegeneration in Drosophila. PLoS Biol. *6*, e29.

Lim, C. and Allada, R. (2013). ATAXIN-2 activates PERIOD translation to sustain circadian rhythms in Drosophila. Science *340*, 875-879.

McCann, C., Holohan, E.E., Das, S., Dervan, A., Larkin, A., Lee, J.A., Rodrigues, V., Parker, R., and Ramaswami, M. (2011). The Ataxin-2 protein is required for microRNA function and synapse-specific long-term olfactory habituation. Proc. Natl. Acad. Sci. U. S. A. *108*, E655-E662.

Nalavadi, V.C., Muddashetty, R.S., Gross, C., and Bassell, G.J. (2012). Dephosphorylation-induced ubiquitination and degradation of FMRP in dendrites: a role in immediate early mGluR-stimulated translation. J. Neurosci. *32*, 2582-2587.

Neumann, M., Sampathu, D.M., Kwong, L.K., Truax, A.C., Micsenyi, M.C., Chou, T.T., Bruce, J., Schuck, T., Grossman, M., Clark, C.M., et al. (2006). Ubiquitinated TDP-43 in frontotemporal lobar degeneration and amyotrophic lateral sclerosis. Science *314*, 130-133.

Nkiliza, A., Mutez, E., Simonin, C., Lepretre, F., Duflot, A., Figeac, M., Villenet, C., Semaille, P., Comptdaer, T., Genet, A., et al. (2016). RNA-binding disturbances as a continuum from spinocerebellar ataxia type 2 to Parkinson disease. Neurobiol. Dis. *96*, 312-322.

Nonhoff, U., Ralser, M., Welzel, F., Piccini, I., Balzereit, D., Yaspo, M.L., Lehrach, H., and Krobitsch, S. (2007). Ataxin-2 interacts with the DEAD/H-box RNA helicase DDX6 and interferes with P-bodies and stress granules. Mol. Biol. Cell *18*, 1385-1396.

Park, J.H., Chung, C.G., Seo, J., Lee, B.H., Lee, Y.S., Kweon, J.H., and Lee, S.B. (2020). C9orf72-associated arginine-rich dipeptide repeat proteins reduce the number of Golgi outposts and dendritic branches in Drosophila neurons. Mol. Cells *43*, 821-830.

Paulson, H.L., Shakkottai, V.G., Clark, H.B., and Orr, H.T. (2017). Polyglutamine spinocerebellar ataxias - from genes to potential treatments. Nat. Rev. Neurosci. *18*, 613-626.

Protter, D.S.W. and Parker, R. (2016). Principles and properties of stress granules. Trends Cell Biol. *26*, 668-679.

Ravanidis, S., Kattan, F.G., and Doxakis, E. (2018). Unraveling the pathways to neuronal homeostasis and disease: mechanistic insights into the role of RNA-binding proteins and associated factors. Int. J. Mol. Sci. *19*, 2280.

Romano, M. and Buratti, E. (2013). Targeting RNA binding proteins involved in neurodegeneration. J. Biomol. Screen. *18*, 967-983.

Satterfield, T.F., Jackson, S.M., and Pallanck, L.J. (2002). A Drosophila homolog of the polyglutamine disease gene SCA2 is a dosage-sensitive regulator of actin filament formation. Genetics *162*, 1687-1702.

Siomi, H., Siomi, M.C., Nussbaum, R.L., and Dreyfuss, G. (1993). The protein product of the fragile X gene, FMR1, has characteristics of an RNA-binding protein. Cell *74*, 291-298.

Sudhakaran, I.P., Hillebrand, J., Dervan, A., Das, S., Holohan, E.E., Hulsmeier, J., Sarov, M., Parker, R., VijayRaghavan, K., and Ramaswami, M. (2014). FMRP and Ataxin-2 function together in long-term olfactory habituation and neuronal translational control. Proc. Natl. Acad. Sci. U. S. A. *111*, E99-E108.

Van Damme, P., Veldink, J.H., van Blitterswijk, M., Corveleyn, A., van Vught, P.W., Thijs, V., Dubois, B., Matthijs, G., van den Berg, L.H., and Robberecht, W. (2011). Expanded ATXN2 CAG repeat size in ALS identifies genetic overlap between ALS and SCA2. Neurology *76*, 2066-2072.

Xu, F., Kula-Eversole, E., Iwanaszko, M., Lim, C., and Allada, R. (2019). Ataxin2 functions via CrebA to mediate Huntingtin toxicity in circadian clock neurons. PLoS Genet. *15*, e1008356.

Yokoshi, M., Li, Q., Yamamoto, M., Okada, H., Suzuki, Y., and Kawahara, Y. (2014). Direct binding of Ataxin-2 to distinct elements in 3' UTRs promotes mRNA stability and protein expression. Mol. Cell *55*, 186-198.

Zhang, Y., Ling, J., Yuan, C., Dubruille, R., and Emery, P. (2013). A role for Drosophila ATX2 in activation of PER translation and circadian behavior. Science *340*, 879-882.